INTERNATIONAL JOURNAL FOR NUMERICAL METHODS IN FLUIDS
Int. J. Numer. Meth. Fluids 2007; **55**:637–653
Published online 21 March 2007 in Wiley InterScience (www.interscience.wiley.com). DOI: 10.1002/fld.1478

Temporal accuracy analysis of phase change convection simulations using the JFNK-SIMPLE algorithm

Katherine J. Evans*, † and Dana A. Knoll‡

T-3, Fluid Dynamics Group, Los Alamos National Laboratory, P.O. Box 1663, MS B216, Los Alamos, NM 87544, U.S.A.

SUMMARY

The incompressible Navier–Stokes and energy conservation equations with phase change effects are applied to two benchmark problems: (1) non-dimensional freezing with convection; and (2) pure gallium melting. Using a Jacobian-free Newton–Krylov (JFNK) fully implicit solution method preconditioned with the SIMPLE (*Numerical Heat Transfer and Fluid Flow*. Hemisphere: New York, 1980) algorithm using centred discretization in space and three-level discretization in time converges with second-order accuracy for these problems. In the case of non-dimensional freezing, the temporal accuracy is sensitive to the choice of velocity attenuation parameter. By comparing to solutions with first-order backward Euler discretization in time, it is shown that the second-order accuracy in time is required to resolve the fine-scale convection structure during early gallium melting. Qualitative discrepancies develop over time for both the first-order temporal discretized simulation using the JFNK-SIMPLE algorithm that converges the nonlinearities and a SIMPLE-based algorithm that converges to a more common mass balance condition. The discrepancies in the JFNK-SIMPLE simulations using only first-order rather than second-order accurate temporal discretization for a given time step size appear to be offset in time.

Received 31 October 2006; Revised 1 February 2007; Accepted 7 February 2007

KEY WORDS: Newton–Krylov methods; temporal accuracy; time step convergence; gallium melting; SIMPLE preconditioner; phase change convection

*Correspondence to: Katherine J. Evans, T-3, Fluid Dynamics Group, Los Alamos National Laboratory, P.O. Box 1663, MS B216, Los Alamos, NM 87544, U.S.A.
†E-mail: kevans@lanl.gov
‡Current affiliation: Nuclear Science and Engineering Division, Idaho National Laboratory, P.O. Box 1625, Idaho Falls, ID 83415, U.S.A.

Contract/grant sponsor: National Nuclear Security Administration; contract/grant number: DE-AC52-06NA25396 (LA-UR-06-7254)

1. INTRODUCTION

Monitoring the phase front during metal castings is important for a complete understanding of the strength and properties of the eventual solid material. Knowledge about convective behaviour in the cooling liquid and its influence on the associated phase front progression over time can assist with quality control. Unfortunately, replication *via* laboratory experiments is virtually impossible to perform. Therefore, accurate simulations of time-dependent phase change convection and front tracking are crucial.

The two-dimensional simulation of melting and solidification of pure metals with convection provides a tractable framework to develop accurate models of phase transitions. Even with these simplifications to the physical system, capturing realistic time-dependent phase change interfaces within convective flow regimes is a challenge. Incorporating convection associated with temperature gradients in the fluid adds a coupling of the momentum and temperature field. Latent heat release and velocity attenuation at the phase front reduces the dynamical time step of the problem. Also, monitoring the location of the phase front requires an accurate tracking method in space and time.

There has been recent focus on the spatial accuracy required for phase change convection simulations. A high aspect ratio natural convection study has discounted lower order spatial discretization methods for being overly diffusive for coarse grid recirculating flows [1]. A reference solution for pure tin melting has been offered using a comprehensive assessment of spatial convergence [2]. A comprehensive look at a gallium melting problem showed visually that sufficiently fine grids and second-order spatial differencing is required to resolve the proper number and location of convective roll cells and the phase front position with time [3]. Of equal importance to adequate spatial resolution is the accuracy of solutions as they progress over time, which has not yet been assessed for phase change convection simulations.

The issue of time accuracy for nonlinear multiphysics problems has been investigated recently in the framework of geophysical flows [4], two-phase flow coupled with heat conduction [5] and radiation diffusion [6]. When multiple scales of physical behaviour are present in time-dependent problems, the physics occurring at the dynamical times scale determines the time step size at which the entire model problem can be solved accurately. In some cases, physical processes occurring at relatively fast time scales have cancelling effects, and a method that can produce stable solutions using larger time step sizes will maintain accuracy. A model of both convection and phase change must either: (1) linearize the equations and take small enough time steps to limit nonlinear effects; or (2) split off the phase change by solving for temperature implicitly separate from other forcings, which are solved explicitly. In this way, the time step can be larger than the Courant–Friedrichs–Lewy (CFL) stability limit of the problem. The CFL, or CFL number, specifies the upper stability limit for time step sizes using explicit methods. As another option, (3) the entire equation set can be solved implicitly to a specified nonlinear tolerance. Although (2), to which is referred as a semi-implicit solution method, and (3) can both produce solutions using higher-order discretizations, it has been demonstrated for a range of problems that additional time integration error terms exist when equations are split and linearized [7].

It has been recently established that the Jacobian-free Newton–Krylov algorithm preconditioned with SIMPLE (JFNK-SIMPLE) is an efficient solution method for two-dimensional phase change convection simulations of a non-dimensional freezing material and pure gallium melting [8]. The JFNK-SIMPLE algorithm solves the nonlinear equation set as in option (3) above. Compared to SIMPLE as a stand-alone solver, JFNK-SIMPLE completed the simulations more quickly for the same time step size and converged using larger time steps for both melting and freezing simulations.

DOI: 10.1002/fld

With this algorithm, significant computational expense has been removed and it is possible to expand on the degree of complexity that has been previously been included in phase change convection problems. However, the temporal accuracy of fully implicit algorithms, especially when compared to the accuracy other more traditional solution methods, is not well understood.

Presently, a comprehensive look at temporal accuracy of phase change convection simulations using the fully implicit JFNK-SIMPLE algorithm is performed using the examples of non-dimensional solidification and pure gallium melting with significant convection structure at early times. These simulations are compared to those using the more traditional SIMPLE algorithm. The model equations and parameters used for the current study are described in Section 2. The nature and convergence criteria of these algorithms are outlined in Section 3. The results and discussion are presented in Section 4 with conclusions in Section 5.

2. MODEL EQUATIONS

The equations of motion governing the model are the time-dependent two-dimensional incompressible Navier–Stokes equations with continuity and thermodynamics. The mathematical representation of phase change is expressed with the enthalpy form of the energy equation including latent heat terms. This allows a single-valued expression of the internal energy of the system and is consistent with earlier work. The resulting equations in non-dimensional form are given by,

$$\frac{\partial u}{\partial t} + \nabla\cdot\mathbf{v}u - \frac{1}{Re}\mathbf{\Delta}u + \frac{1}{\rho}\frac{\partial p}{\partial x} - A(H)u = 0 \tag{1}$$

$$\frac{\partial v}{\partial t} + \nabla\cdot\mathbf{v}v - \frac{1}{Re}\mathbf{\Delta}v + \frac{1}{\rho}\frac{\partial p}{\partial y} - A(H)v = f_v \tag{2}$$

$$\nabla\cdot\mathbf{v} = 0 \tag{3}$$

$$\frac{\partial H}{\partial t} + \nabla\cdot\mathbf{v}H + \frac{c_p}{Re\,Pr}\mathbf{\Delta}\tau(H) = 0 \tag{4}$$

where the dependent variables are the horizontal and vertical velocities $\mathbf{v} = \{u, v\}$, pressure (p), and total enthalpy (H). These variables combine to make up the state vector $\mathbf{x} = \{u, v, p, H\}^{\mathrm{T}}$ to be solved at each time step. The term $\tau(H)$ in Equation (4) is the temperature function expressed solely in terms of H defined below. The symbols $\mathbf{\Delta}$ and $\nabla\cdot$ represent the two-dimensional Laplacian and divergence operators, respectively. Additional parameters that define the system are the density ρ, latent heat L, specific heat c_p, Prandtl number Pr, Reynolds number Re, and Rayleigh number Ra. For this study, the temperature range is small, so c_p and ρ are set constant between phases. Equations (1)–(4) are discretized using second-order centred differencing in space. For time discretization, two fully implicit options have been implemented: (1) first-order backward-Euler (BE); and (2) second-order backward difference formula (BDF2), and are discussed in detail in Section 3.3.

The velocity attenuation (commencement) as the material solidifies (liquifies) in the region of the domain is treated with a forcing term in the momentum equation, $A(H)\mathbf{v}$. Because we are simulating pure material behaviour, a simple linear relationship to the solid fraction of the material is used to damp the material velocity in the vicinity of the phase front, so $A(H) = A'\varepsilon_s$. The constant A' is based on the thermodynamic properties of the simulation and ε_s is the solid fraction

DOI: 10.1002/fld

of the material. The material in the domain is either solid ($\varepsilon_s = 1$), liquid ($\varepsilon_s = 0$), or within a numerical mushy zone ($0 \leqslant \varepsilon_s \leqslant 1$), the region where a portion of the latent heat has been released or absorbed. The buoyancy force acting on the fluid arises from the Boussinesq approximation, which is given by $\mathbf{f}(H) = \{f_u = 0,\ f_v = (Ra/Re^2\, Pr)\tau(H)\}$.

Presently, energy conservation is expressed in terms of total enthalpy

$$H = c_p T + (1 - \varepsilon_s)L \tag{5}$$

and accounts for energy changes associated with a change in temperature (T) and phase. For a pure material, the temperature can be extracted from H using

$$T = \tau(H) = \begin{cases} H/c_p & \text{if } H < c_p T_m \\ T_m & \text{if } c_p T_m \leqslant H \leqslant c_p T_m + L \\ (H - L)/c_p & \text{if } H > c_p T_m + L \end{cases}$$

where T_m is the melting temperature. The domain is defined spatially using a finite volume two-dimensional Cartesian staggered fixed grid, whereby p and H lie at the cell centres and u and v lie on the western and southern cell faces, respectively. The domain consists of a rectangular cavity of equal-sized cells along each direction, $\Omega = [0 : b_x, 0 : b_y]$ with boundary conditions of

$$u = v = 0 \quad \text{on } \partial\Omega \tag{6}$$

$$H(0, y) = H_l, \quad H(b_x, y) = H_r, \quad y \in [0, b_y] \tag{7}$$

$$\frac{\partial H}{\partial y}(x, 0) = \frac{\partial H}{\partial x}(x, b_y) = 0, \quad x \in [0, b_x] \tag{8}$$

This corresponds to insulating top and bottom walls and left (H_l) and right (H_r) sidewalls with a specified constant value. As mentioned, latent heat release associated with liquid to solid phase change is tracked directly within the enthalpy framework. This model framework provides a direct comparison with the majority of recent phase change models.

3. SOLUTION ALGORITHMS

In this analysis, two algorithms are employed to investigate algorithm accuracy, the SIMPLE algorithm and the JFNK solver. These algorithms as applied to phase change convection problems are outlined in a recent study of algorithm efficiency [8], and will therefore only be summarized below. Both algorithms are employed for this study because they naturally lend themselves to the convergence criteria to which they are being solved. The SIMPLE algorithm could be converged to the same tighter tolerance as JFNK-SIMPLE, but used this way as it is much less robust along the range of time step sizes used here. However, it is a common solution method for problems with phase transition and provides a parallel comparison with earlier work.

3.1. SIMPLE algorithm

SIMPLE is a nested linear iterative process commonly used for coupled problems of momentum and energy [9]. Linear stationary solution methods are applied for a set number of sweeps to

DOI: 10.1002/fld

generate approximate updates of each dependent variable, which are then used to correct for mass balance through pressure and momentum corrections. In this application of SIMPLE, an update to the enthalpy equation is generated using 20 sweeps of the successive over-relaxation method. The frozen enthalpy update is then used in 10 sweeps to generate an update of u and v sequentially using Gauss–Seidel. The momentum updates provide an input to generate δp using Equation (3) which is fed back into the momentum equations to produce a velocity correction. This brings the system towards mass balance. The 'mass balance' condition as a convergence criterion is set to $\delta p \leqslant 1 \times 10^{-5}$ and δu and $\delta v \leqslant 1 \times 10^{-2}$ to be consistent with traditional SIMPLE convergence characteristics [3, 10]. The SIMPLE update of pressure is damped by a factor $\alpha = 0.2$ to account for an overestimation of the velocity correction (refer to [9]). When applied as a preconditioner, the set of sweeps through all the equations and the velocity corrections is repeated for a set of cycles, the number of which depends on factors such as the spatial and temporal scales of the problem. When used as the main solver, the convergence test was performed after each set of sweeps through the individual line solves. As an alternative to the mass balance convergence criterion, the SIMPLE algorithm could employ a full nonlinear norm reduction as the convergence criterion. However, there is no tolerance test after a specified number of sweeps and limited coupling of the equations, so the efficiency and robustness of the algorithm used in this way are limited [8]. For convergence defined as a reduction of the nonlinear norm, we use the JFNK-SIMPLE algorithm presented in Section 3.2.

3.2. JFNK preconditioned with SIMPLE

The JFNK algorithm is a nested iteration solution method consisting of an outer nonlinear loop, inside which a linear solver calculates an approximate solution guess. To minimize the work of the linear solver, a preconditioner based on the SIMPLE algorithm is employed. A general discussion of JFNK is presented in a recent review article [11]. The details of JFNK-SIMPLE as applied here are outlined in Evans *et al.* [8] and will only be summarized here. The outer loop solves the full nonlinear equation set (1)–(4) in residual form

$$\mathbf{F}(\mathbf{x}) = 0 \tag{9}$$

where $\mathbf{F}$ is the function of nonlinear residuals for each dependent variable in $\mathbf{x}$. A solution is found at the time advanced solution by minimizing $\mathbf{F}(\mathbf{x})$. A first-order Taylor series expansion of $\mathbf{F}(\mathbf{x})$ in (9) gives

$$\mathbf{J}(\mathbf{x}^k)\delta\mathbf{x}^k = -\mathbf{F}(\mathbf{x}^k), \quad \mathbf{x}^{k+1} = \mathbf{x}^k + \delta\mathbf{x}^k \tag{10}$$

where $\mathbf{J}$ is the Jacobian for $\mathbf{F}$ and k is the nonlinear iteration index. A specified drop of the L_2 norm of the residual η_{nl} defines nonlinear convergence

$$\frac{\|\mathbf{F}(\mathbf{x}^k)\|_2}{\|\mathbf{F}(\mathbf{x}^o)\|_2} < \eta_{\mathrm{nl}} \tag{11}$$

which is set to $\eta_{\mathrm{nl}} = 1 \times 10^{-8}$ for error calculations, and $\eta_{\mathrm{nl}} = 1 \times 10^{-6}$ elsewhere.

The nonlinear Newton loop of JFNK receives a linear approximation to the nonlinear equation set (9) from generalized minimum residual (GMRES), a Krylov method that utilizes least squares to maximize the quality of the update for non-symmetric problems. Rather than forming the Jacobian

DOI: 10.1002/fld

directly, a finite-difference approximation of the Jacobian times a vector is formed

$$\mathbf{Jv} \simeq \frac{\mathbf{F}(\mathbf{x} + \varepsilon\mathbf{v}) - \mathbf{F}(\mathbf{x})}{\varepsilon} \tag{12}$$

where ε is a small perturbation. The Jacobian-vector product is used to update the Krylov vector in the linear iterative process until the linear update satisfies

$$\frac{\|\mathbf{J}\delta\mathbf{x}^k + \mathbf{F}(\mathbf{x}^k)\|_2}{\|\mathbf{F}(\mathbf{x}^k)\|_2} < \eta_k \tag{13}$$

The setting of η_k, which is the linear tolerance parameter, varies depending on the type of problem to be solved. For the time-dependent problems with some significant nonlinearity, a constant value of $\eta_k = 1 \times 10^{-2}$ maximizes efficiency of the overall algorithm. The $\delta\mathbf{x}$ update in (13) is determined from the most recent Krylov vector, and the vector grows with each linear loop. To minimize the number of linear GMRES loops and the associated storage costs, $\delta\mathbf{x}$ is generated with the use of a preconditioner.

Presently, the SIMPLE algorithm is used as a physics-based preconditioner to JFNK. The term 'physics-based' refers to the use of a simplified form of the original discretized nonlinear equation set. Choosing appropriate simplifications maximizes the effect of the preconditioner to produce a quality linear solution update within JFNK. The 'right' preconditioning option is implemented in the left equation of (10) for a time step k as

$$\mathbf{J}(\mathbf{M}^{-1}\delta\mathbf{z}) = -\mathbf{F}(\mathbf{x}) \tag{14}$$

where $\mathbf{M}^{-1}$ is the preconditioning operator expressed in matrix form and $\delta\mathbf{z} = \mathbf{M}\,\delta\mathbf{x}$. Note that $\mathbf{M}$ itself is never required, rather $\mathbf{M}^{-1}$ is called in two places within the algorithm in the process of generating a linear update $\delta\mathbf{x}$ in the Krylov loop. First, a set of calls is performed to calculate $\mathbf{M}^{-1}\delta\mathbf{z}$ which builds the Krylov vector. Once the Krylov vector meets the convergence criteria, a single call is made to return $\delta\mathbf{x}$ for Equation (13). Although the preconditioner is displayed here in matrix form, it is more precisely defined as an approximate inverse to the original equations.

The preconditioner $\mathbf{M}^{-1}$ is approximated through a prescribed number of sweeps of the SIMPLE algorithm as described in Section 3.1. As a physics-based preconditioner to JFNK, SIMPLE is applied with three simplifications to the phase change convection model equation set: (1) first-order upwind spatial differencing is used to calculate advection and diffusion terms; (2) the amount of latent heat released within a control volume changing phase is held constant during the construction of $\mathbf{M}^{-1}$; and (3) first-order discretization in time is used. Because this analysis is restricted to a pure material, step (2) is equivalent to holding control volumes to the current phase while in the preconditioner portion of the algorithm. Note that the velocity attenuation is still applied to the preconditioner algorithm, but no new attenuation due to phase change occurs. None of these changes affect the accuracy of the solution, only the efficiency at which an linear update within the specified tolerance for (13) is found.

3.3. Temporal discretization of variables

The discretization of the time derivatives is a key component of this temporal accuracy analysis. The model equations (1)–(4) can be written such that $\boldsymbol{\phi}$ is any variable within the state vector $\mathbf{x}$ and $\boldsymbol{\phi}_s$ is the spatial discretization of $\boldsymbol{\phi}$. Because these are coupled equations, $\boldsymbol{\phi}_s$ encompasses

DOI: 10.1002/fld

more than one variable within **x** in some cases. The first-order accurate discretization in time used here is the fully implicit BE method

$$\boldsymbol{\phi}^{n+1} = \boldsymbol{\phi}^{n} + \boldsymbol{\phi}_{\mathrm{s}}^{n+1}\Delta t \tag{15}$$

The superscript $n+1$ is the new time level, n is the current time level, and Δt denotes the time step size, which is constant for this study. For fully implicit methods, the appropriate time step size (within reason) is governed by accuracy rather than stability.

The second-order time discretization used here is BDF2 [12], which is a three-level fully implicit scheme given by

$$\boldsymbol{\phi}^{n+1} = \boldsymbol{\phi}^{n} + \tfrac{1}{3}(\boldsymbol{\phi}^{n} - \boldsymbol{\phi}^{n-1}) + \tfrac{2}{3}\boldsymbol{\phi}_{\mathrm{s}}^{n+1}\Delta t \tag{16}$$

for a constant time step size. BDF2 uses information from the $n+1$, n, and $n-1$ time levels, which prevents oscillatory behaviour sometimes present with large time steps in centred difference type temporal schemes such as Crank–Nicolson.

4. RESULTS

In order to compare algorithm accuracy directly with earlier modelling studies, we have selected two benchmark problems of time-dependent convection with phase transitions. The equations outlined in Section 2 are applied to a non-dimensional solidification problem in a square cavity (Section 4.1), and a pure gallium melting problem (Section 4.2). The parameters of both problems are presented in Table I. Recent work has computed solutions to the same problems to analyse algorithm efficiency [8, 13].

The present study is focused on the accuracy of solutions to these problems given: (1) a convergence criteria set for the nonlinear discretized equations for a given time step; (2) time step size; and (3) the temporal discretization of the model equations. Spatial accuracy is vitally important

Table I. Parameters and domain configuration for non-dimensional solidification within a square cavity (Problem 1) and gallium melting within a rectangular cavity (Problem 2).

Parameter	Symbol	Units (Prob 2)	Problem 1	Problem 2
Domain width	$[0 : b_x]$	m	[0 : 4]	[0 : 0.0356]
Domain height	$[0 : b_y]$	m	[0 : 4]	[0 : 0.0635]
Rayleigh #	Ra	ND	3×10^3	7.0×10^5
Latent heat	L	J/kg	1.0	8.016×10^4
Specific heat	c_p	J/kg/K	1.0	381.5
Prandtl #	Pr	ND	1.0	0.0216
Reynolds #	Re	ND	1.0	3.37×10^6
Density #	ρ	$\mathrm{kg/m^3}$	1.0	6.093×10^3
Melt temperature	T_{m}	K	0.0	302.78
Right wall temperature	T_{r}	K	0.5	301.0
Left wall temperature	T_{l}	K	−0.5	311.0
Velocity attenuation	A'	$\mathrm{s^{-1}}$	1.56×10^3	1.56×10^9

'ND' refers to a non-dimensional value and the melt, left, and right wall temperature values are converted to enthalpy when implemented.

DOI: 10.1002/fld

as well, but has been addressed in previous related numerical studies of spatial refinement [3, 14] and discretization [1]. Wherever possible within the scope of this study, those findings have been incorporated. When the convergence criterion is set to a 'mass balance' condition, the SIMPLE algorithm (Section 3.1) is used. In this case, simulations converged to mass balance using the SIMPLE algorithm are discretized to first order in time using BE explained in Section 3.3. When a 'nonlinear' convergence is specified, this refers to the convergence of the full discretized equations (1)–(4) to a global L_2 norm using the JFNK-SIMPLE algorithm (Section 3.2). The solutions found using the nonlinear convergence criterion are either first- or second-order discretized, using (15) or (16), respectively.

4.1. Non-dimensional solidification

The solidification of a fluid undergoing natural convection in a square cavity is simulated. This problem is very similar to earlier benchmark problems [15–17]. At time $= 0$, the cavity contains a fluid at rest at temperature $T = +0.5$, which is above the freezing point of $T_m = 0.0$. The left and right walls of the domain are set constant at $T = -0.5$ and $T = +0.5$, respectively. Additional parameters are given in Table I. The simulation is run to time $= 100$ to ensure sufficient solidification on the left but minimize computational time, and the solution is presented in Figure 1. As expected, the hot and cold walls induce an anticyclonic circulation whereby colder fluid is advected further into the domain at the bottom. As a result, the phase front has two-dimensional structure as the freezing progresses from left to right. To discern the temporal error, the simulations are performed with varying time step sizes using three different accuracy criteria; nonlinear convergence with: (1) first-order BE discretization; (2) second-order BDF2; and (3) convergence to mass balance using BE. The temporal accuracy of these runs can be calculated quantitatively by determining

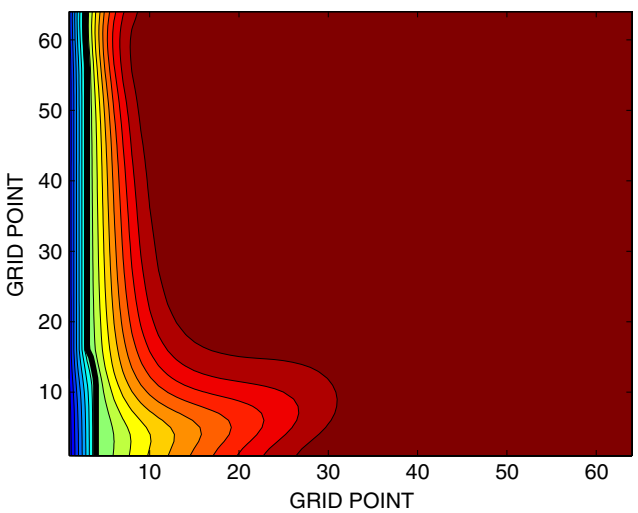

Figure 1. Temperature contours for solution to a non-dimensional freezing problem with parameters as given in Table I after 100 s on a 64^2 grid. The thick black line denotes the phase front contour at $T = 0.0$ and red indicates warmer temperatures.

DOI: 10.1002/fld

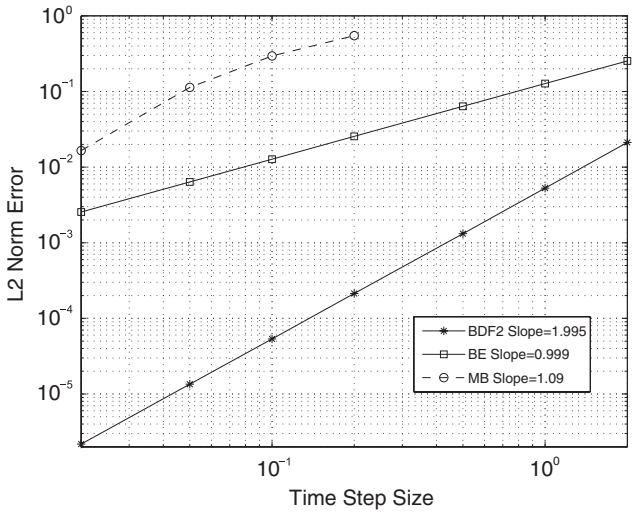

Figure 2. L_2 norm of error of enthalpy (H) for non-dimensional solidification after 100 s on a 32^2 compared to a base run using a time step size $t = 1 \times 10^{-3}$. The number beside each parameter label provides the slope of the temporal error line, which is the order of error.

the L_2 norm of error of the enthalpy (H) field from a reference solution. A reference solution can be determined many ways; because there is no analytical solution from which to compare, the reference solution used here is calculated from a relatively very small time step of 1×10^{-3} using BDF2 and a nonlinear tolerance of $\eta_{\text{nl}} = 1 \times 10^{-8}$. These norms are plotted on a log–log scale in Figure 2, and the slope of the line connecting the error of simulations performed with the same temporal discretization provides the order of error. This provides a relative temporal accuracy analysis. The first-order nonlinearly converged simulations are displayed with the solid line with square markers and exhibit a robust first-order error (slope = 0.99). The same simulations with second-order discretization are displayed as the solid starred line and demonstrate a robust second-order error (slope = 1.995). Note that these runs range from a time step size of 0.02–2, which is close to the CFL number for this problem. The fully implicit JFNK-SIMPLE algorithm can converge with time step sizes that produce a CFL number above 1.0; however, the accuracy of stepping over the time scale of the flow may be unacceptably high.

The dashed line with circle markers in Figure 2 indicates solutions converged to the mass balance condition with BE discretization. Above a time step size of 0.2, the SIMPLE algorithm could not converge to the mass balance criteria. Even though the equations are discretized using first-order BE discretization, the error of the simulation was not first-order accurate over the range of time steps of the study. At larger time steps, the error is below first-order accurate and qualitative differences in the temperature contours from simulations used to produce Figure 2 are present. Additional sweeps through SIMPLE for each time step reduce the error, but it is unable to match the nonlinearly converged BE solutions generated using JFNK-SIMPLE for this simulation. For example, at a time step size of 0.5, 50 sweeps of SIMPLE produces a converged solution, but with an error of 0.083 *versus* 0.064 with JFNK-SIMPLE.

A time step convergence analysis similar to the one presented in Figure 2 was performed for various values of the velocity parameter A' in Equations (1) and (2) on a 32^2 grid. A base

DOI: 10.1002/fld

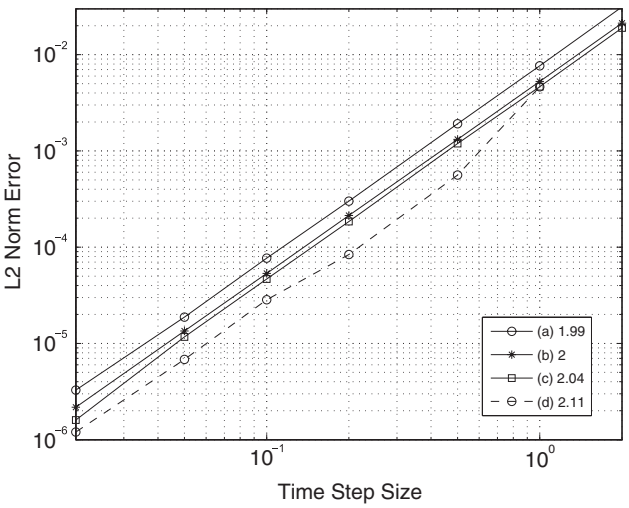

Figure 3. Convergence of the global norm of enthalpy (H) for non-dimensional solidification (after 100 s) for various velocity attenuation parameters (a)–(d) as outlined in the text. The number beside each parameter label provides the slope of the error line.

run was created for a range of attenuation parameters: (a) $A' = 1.56 \times 10^2$; (b) $A' = 1.56 \times 10^3$; (c) $A' = 1.56 \times 10^4$; and (d) $A' = 1.56 \times 10^6$, using the same convergence parameters as for the analysis in Figure 2 for nonlinear convergence with BDF2 discretization. Then, corresponding runs with larger time steps were performed and compared to the base run with the same value of A'. The error for each parameter setting is plotted in Figure 3. Simulations with values (a)–(c) converge with second-order accuracy over the range of time scales presented, but with different L_2 norms of error for a given time step. As the attenuation parameter is increased, the equations become more stiff and convergence becomes more difficult. However, the more strongly damped velocities produced with the higher attenuation parameter results in a slightly lower error because there is less variation in the phase front location as the time step is increased. For the simulations where the parameter is set to (c) and (d), the number of sweeps through the preconditioner is increased from 5 to 10 to achieve consistent convergence, which retards efficiency. Referring to Figure 3, convergence above a time step size of 1.0 for (d) is not possible even with these alterations. Further, the robust second-order accuracy achieved with the smaller attenuation values is no longer present.

For this non-dimensional freezing problem, the error associated with different settings of the velocity attenuation term (represented by the difference between the lines in Figure 3) is a conceptually different kind of error than the temporal error investigated here and is beyond the scope of the study (see [17, 18] for more discussion). The salient point to gain from Figure 3 is that different choices of the velocity attenuation parameter affect how well the JFNK-SIMPLE algorithm produces robust second-order nonlinearly converged solutions. The goal is to choose the velocity damping term that fully extinguishes the velocities in the solid region but still provides robust convergence criteria. Obviously, for simulations of actual materials, the attenuation term that most closely matches the material properties and observed solidification behaviour is desired. The solutions from the simulations used to generate Figure 3 are presented in Figure 4. Figure 4 is analogous to Figure 1, but focused on the left fifth portion of the domain with the freezing front

DOI: 10.1002/fld

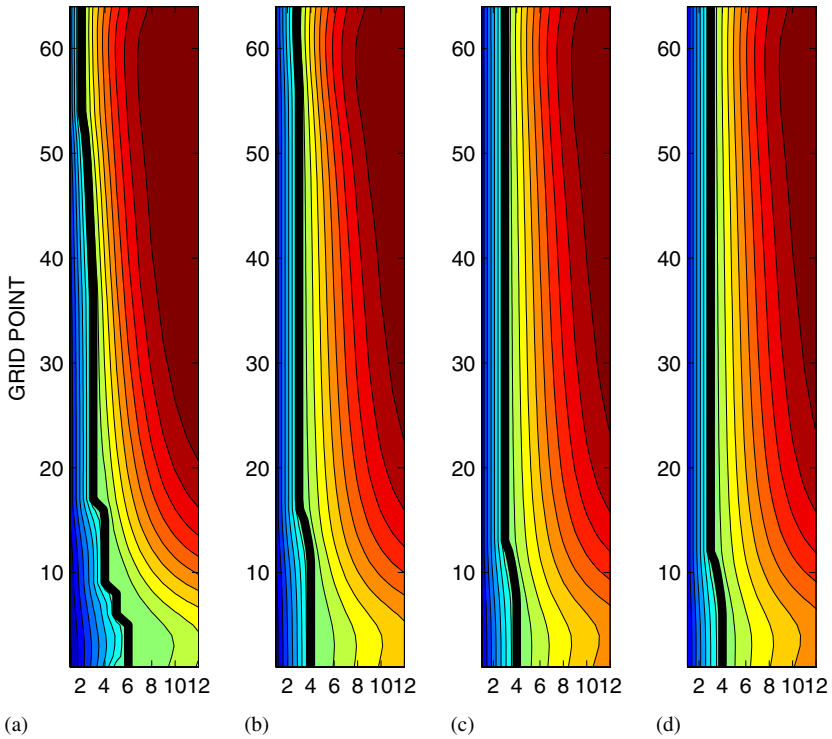

Figure 4. Temperature contours for the solution to a non-dimensional freezing problem after 100 s on a 64^2 grid, matching Figure 1 except only the left fifth of the domain is shown for emphasis. The thick black line denotes the phase front contour at $T = 0.0$. Various velocity attenuation parameters: (a) $A' = 1.56 \times 10^2$; (b) $A' = 1.56 \times 10^3$; (c) $A' = 1.56 \times 10^4$; and (d) $A' = 1.56 \times 10^6$ are used.

to show detail. When A' is set to (a), the velocity is not damped sufficiently because the frozen material is still being advected. For (b), the material is basically stationary in the frozen region. With (c) and (d) settings, the velocity is still extinguished at the front as desired, but converging the JFNK-SIMPLE algorithm to the same criteria requires more effort by the algorithm for the equations are more stiff. Nonetheless, the JFNK-SIMPLE algorithm can still converge the solution very close to second-order accuracy.

4.2. Gallium melting

The model described in Section 2 is also used to find solutions for the early melting of gallium. Gallium is considered a benchmark problem for numerical analyses; very limited experimental data are available [19] and a body of previous modelling studies have been performed from which to compare (e.g. [3, 10, 16]). The parameters used for the gallium melting simulation match actual gallium properties as much as possible given the simplifications of the model, and are presented in Table I. The present domain is matched to the left two-fifths of the domain used in Hannoun *et al.* [3], because the current focus is on early melting. The material is initially solid at

DOI: 10.1002/fld

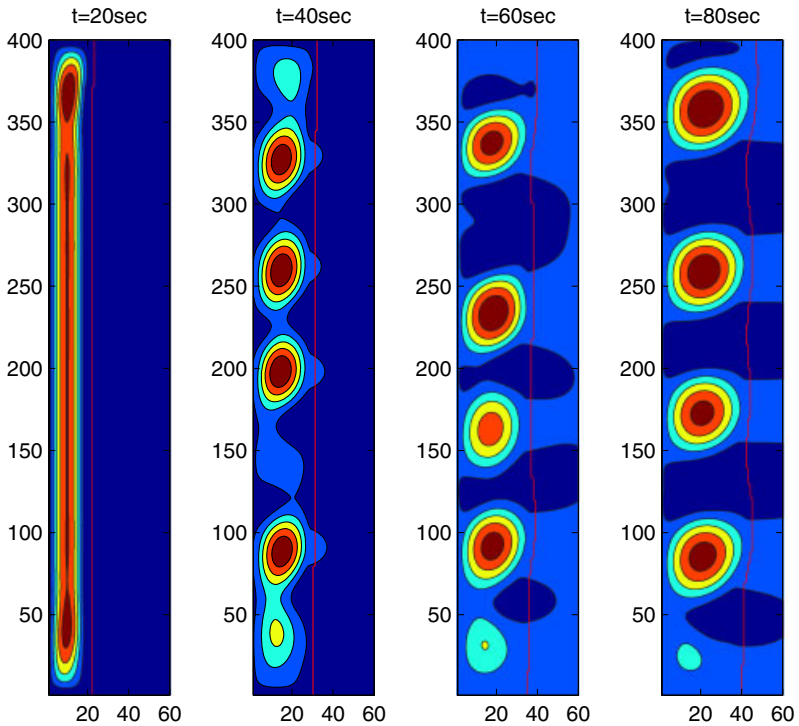

Figure 5. Melting and convection of pure gallium in a 160×400 grid every 20 s with time step of 0.02 s and parameters as in Table I. For clarity, only the left quarter of the domain is displayed. Contours are values of streamfunction and the red line denotes the frozen contour of temperature ($T = 302.77$ K).

301°C, and at time = 0 the left wall of the domain is set at 311°C, which is considerably above the melting temperature of 302.77°C. At subsequent times, the left edge of material in the domain has melted and is flowing. These simulations have been performed on a 160×400 point grid for 80 s using JFNK-SIMPLE with a nonlinear convergence criteria and second-order BDF2 discretization in time. The resulting streamfunction contours are displayed every 20 s in Figure 5. During this simulation, the aspect ratio of the melted region of the left edge of the domain is high, so shear instabilities and multiple convection cells develop. Where possible to compare, these plots closely match the plots produced in a spatial convergence study by Hannoun *et al.* [3]. Our reduced domain size results in a slightly stronger temperature gradient through the solid portion because right edge cold temperature is closer to the melted region.

Hannoun *et al.* [3] determined visually that 240×600 grid spacing (interpolated) was the coarsest grid with adequate spatial resolution. However, the 160×400 and 80×200 grids used for the analyses presented below produced results quite close to the finer grid results presented in [3] when run with a time step converged solution method and using second-order discretization in time. The implications of these differences are discussed below. It is desirable to perform all the temporal accuracy analyses using very fine grids to quantify the error in space and time together. For this analysis, the focus is on temporal error independent from spatial error, so the finest grid that

DOI: 10.1002/fld

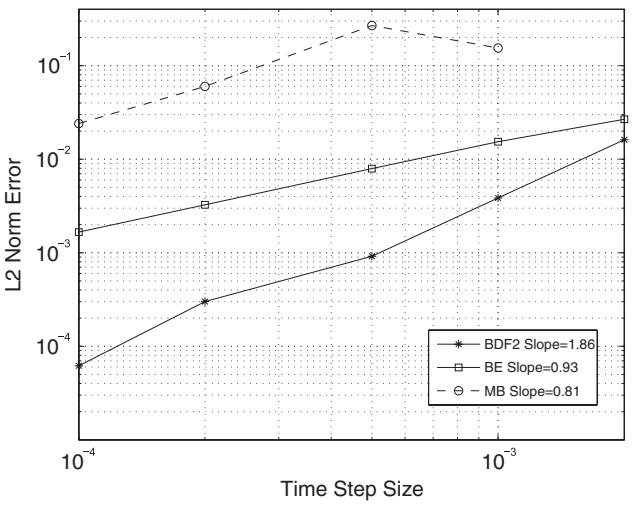

Figure 6. L_2 norm of error of enthalpy (H) for gallium melting after 1 s on a 80×200 grid compared to a base run using a time step size $t = 1 \times 10^{-5}$ and as specified in the text. The labels have the same meaning as in Figure 2.

can perform baseline simulations in a reasonable amount of time is used. For general simulations, where base runs at small time step sizes below the required level for accuracy are not required (as explained below), finer grids are tractable such as in Figure 5.

From Figure 5, it is clear that the cellular-shaped convection is altering the shape of the phase front over time. Just as with spatial accuracy, insufficient resolution of the time evolution of the front may result in qualitative discrepancies in the final solution. To evaluate this effect, a time step convergence study of the gallium melting simulation is performed, analogous to Figure 2 for non-dimensional solidification, to discern the temporal discretization error. The reference solution is calculated using a time step of $\Delta t = 1 \times 10^{-5}$ using BDF2 and a nonlinear tolerance of $\eta_{\mathrm{nl}} = 1 \times 10^{-8}$. As with the analysis above, the temporal accuracy of these runs is determined quantitatively by determining the L_2 norm of error of each simulation from the reference solution. Figure 6 displays the error for JFNK-SIMPLE with BE and BDF2 discretizations and SIMPLE algorithms as described above. These error analyses are performed on a 80×200 grid, however, they were also performed on 40×100 grid (not shown) to test robustness, and the results were consistent. For a range of time step sizes, the JFNK-SIMPLE algorithm captures the model equations with first- and second-order accuracy using BE and BDF2 discretization, respectively. At a time step of 0.002 s, which lies at the points at the right end of the figure, using BDF2 produces almost as much error as using BE. However, by halving the time step to 0.001 s, BDF2 is as accurate as using BE with a time step size that is an order of magnitude smaller. This results in a more efficient algorithm for a given level of accuracy. For example, if the simulation requires that the temporal accuracy be less than about 3×10^{-3} (which is shown below to be required for this gallium melting problem), then using BDF2 completes the simulation 6.3 times faster. When the same simulation is completed with SIMPLE converged to a mass balance condition, it does not converge above a time step size of 1×10^{-3} s. It is not time step converged for time step sizes above 5×10^{-4} s, and the relative error is still above JFNK-SIMPLE run with a time step size 20

DOI: 10.1002/fld

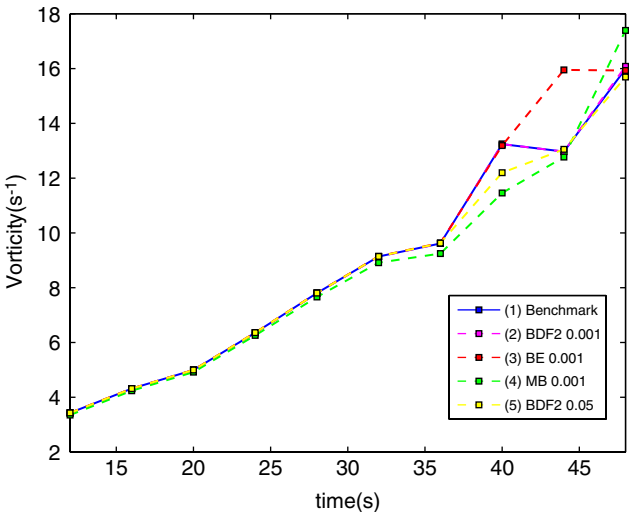

Figure 7. Maximum vorticity within a cavity for a set of simulations of melted pure gallium on a 80×200 grid domain every 4 s. Results at 12–48 s are displayed.

times larger. Although the less restrictive mass balance convergence criteria produces a solution at a given time step more quickly, it is demonstrated below that the loss in accuracy is qualitatively significant.

To illustrate the effects on accuracy by using: (1) large time step sizes; (2) first-order discretization in time; and (3) a mass balance convergence condition using the SIMPLE solver *versus* more rigorous algorithm constraints, the maximum vorticity in the cavity over time is tracked. The vorticity maximum corresponds to the value of vorticity at the centre of the strongest circulation cell in the melted region. Figure 7 displays the maximum vorticity in the cavity for a range of simulations every 4 s from 12 to 48 s. These simulations are compared to a second-order BDF2 nonlinearly converged (JFNK-SIMPLE) solution with a time step of 2.5×10^{-4} s as a time converged benchmark [simulation (1)]. The other simulations include a time step size of 1×10^{-3} s, nonlinearly converged using (2) BDF2 and (3) BE, and (4) BE with a mass balance convergence criterion. As an illustration of the stability of fully implicit JFNK-SIMPLE, simulations with a time step of 0.05 s using BDF2 (5) and BE (5a—not shown) are performed as well. For consistency with Figure 6, these are also presented on a 80×200 grid. At early times, the maximum vorticity of each varies little. However, by about 32 s, the mass balance solution (4) in particular is diverging from the benchmark (1) maximum vorticity value as the simulation progresses.

Up until about 40s, the nonlinearly converged simulations predict very similar maximum vorticity values. At 40 s, however, there are significant differences between simulation (5) from (1)–(3), which match very closely. At 44 s, a significant divergence in the maximum vorticity occurs with simulation (3), which is then virtually eliminated by 48 s. To investigate this discrepancy in more detail, streamfunction contours of the solution at 44 s (Figure 8) and 48 s (Figure 9) are displayed for simulations (1)–(5). Note that only the left quarter of the domain is displayed and expanded in the x direction to enhance detail. Figure 8 shows that at 44 s, the simulations produce flow patterns with some qualitative differences from the time converged benchmark (1). Simulation (2)

DOI: 10.1002/fld

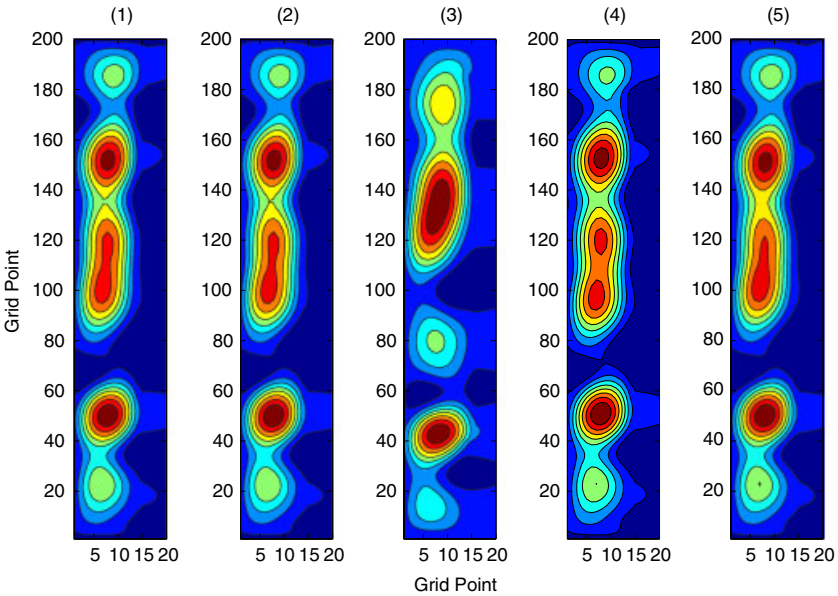

Figure 8. Stream function contours for gallium melting solution at 44 s on an 80×200 grid for simulations (1)–(5) as described in the text.

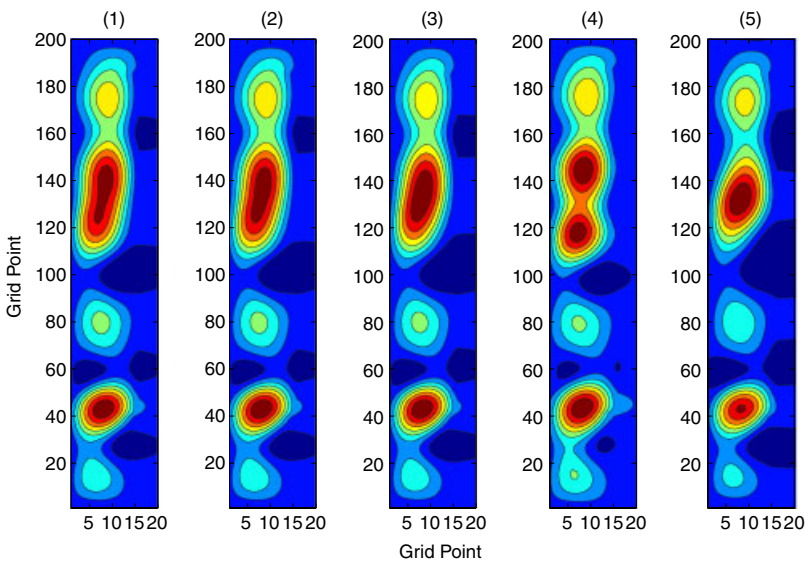

Figure 9. Stream function contours for gallium melting solution at 48 s on an 80×200 grid for simulations (1)–(5) as described in the text.

DOI: 10.1002/fld

has the lowest temporal error (refer to Figure 6) and produces a solution correspondingly close to (1). Simulation (5), which is second-order accurate but uses a large time step size, is also very close. The mass balance converged run (4) is qualitatively different; it has not completely merged two distinct cells present in all the simulations at 40 s (not shown).

As implied in Figure 7, simulation (3) is qualitatively different from the other simulations at 44 s. Figures 8 and 9 provide some insight. It is clear that between 44 and 48 s, two major cells merge into one cell as melting progresses. This merging process has been seen in other melting scenarios as the phase front widens the melt region over time [3, 14]. At 48 s, the circulation cells more closely match the cell pattern seen at 44 s with simulation (3). It appears that the BE nonlinearly converged case is not so much qualitatively different in space but instead has mistimed the roll merging. By 48 s, Figure 9 shows that for all but the mass balanced converged simulation (4), there is one large cell flanked by three smaller circulation cells. This appears to be a temporal rather than spatial discrepancy. Conversely, the mass balance converged simulation (4) continues to produce a solution with the wrong number of distinct circulation cells at 48 s for this grid resolution. The larger time step simulation (5) has discrepancies in terms of circulation strength, but the solution is not as qualitatively different as with (4).

Fully implicit nonlinearly converged methods allow larger time steps to be used for simulations as compared to semi-implicit methods (SIMPLE) or explicit methods, but it is only one algorithmic component. Even with a nonlinear convergence criterion, the JFNK-SIMPLE simulation with first-order discretization (3) cannot produce an accurate result for early gallium melting. With a time step size 50 times larger than the time converged solution, simulation (5) produces a solution with deficiencies. However, the gross circulation features are maintained, which makes the larger time step sizes ideal for probing algorithm characteristics. For accuracy considerations of this problem, a time step converged time step size ($\approx 1 \times 10^{-3}$ s), higher order time discretization such as BDF2, and a solution method that converges the nonlinearities of the discrete model are *all* required to get an accurate solution for early gallium melting.

5. CONCLUSIONS

For phase transition with convection, a number of numerical issues that impact simulation accuracy have been probed. The convergence criterion of the algorithm, the treatment of the velocity attenuation in the phase transition region in the model equations, the order of temporal discretization, and the time step size all influence the ability of the algorithm to be able to match a simulation benchmark. A careful consideration of the velocity attenuation parameter is needed to match the solidification of the material being modelled and minimize the stiffness of the discrete equations. Note that the velocity attenuation parameter setting is less sensitive in the melting case than solidification, likely because the velocity acceleration from zero has less impact on the front location. For the gallium melting problem, temporal accuracy is a crucial component for a qualitatively correct solution. The JFNK-SIMPLE algorithm that converges the nonlinearities with BDF2 discretization demonstrates second-order temporal accuracy. Compared to first-order BE discretization and the SIMPLE algorithm converged to a traditional mass balance condition at a time step converged time step size, it is a superior algorithm.

JFNK-SIMPLE provides the efficiency and accuracy required to proceed forward with more realistic configurations and forcings. Several future directions with this algorithm include adding a concentration equation and mushy zone to be able to simulate the phase change convection

DOI: 10.1002/fld

behaviour of alloys and saltwater sea–ice applications within a fully implicit time converged framework. Temporal accuracy in these cases is needed to capture anisotropies in the concentration of solute and solid material during phase transition, leading to possible macrosegregation and regional ocean circulation transients, respectively. In this case, thermal and solutal buoyancy will provide the forcing for convection and interface structure. Basic double diffusive convection problems and problems with a more complex frontal boundary require the fidelity of the second-order JFNK-SIMPLE algorithm employed here.

ACKNOWLEDGEMENTS

This work was carried out under the auspices of the National Nuclear Security Administration of the U.S. Department of Energy at Los Alamos National Laboratory under Contract No. DE-AC52-06NA25396 (LA-UR-06-7254).

REFERENCES

1. Leonard BP, Drummond JE. Why you should not use 'hybrid', 'power-law', or related exponential schemes for convective modeling—there are much better alternatives. *International Journal for Numerical Methods in Fluids* 1995; **20**:421–442.
2. Hannoun N, Alexiades V, Mai TZ. A reference solution for phase change with convection. *International Journal for Numerical Methods in Fluids* 2005; **48**:1283–1308.
3. Hannoun N, Alexiades V, Mai TZ. Resolving the controversy over tin and gallium melting in a rectangular cavity heated from the side. *Numerical Heat Transfer B* 2003; **44**:253–276.
4. Mousseau VA, Knoll DA, Reisner JM. An implicit nonlinearly consistent method for the two-dimensional shallow-water equations with Coriolis force. *Monthly Weather Review* 2002; **130**:2611–2625.
5. Mousseau VA. A fully implicit hybrid solution method for a two phase thermal-hydraulic model. *Journal of Heat Transfer* 2005; **127**:531–539.
6. Rauenzahn R, Mousseau VA, Knoll DA. Temporal accuracy of the nonequilibrium radiation diffusion equations employing a Saha ionization model. *Computer Physics Communications* 2005; **172**:109–118.
7. Knoll DA, Chacon L, Margolin L, Mousseau V. On balanced approximations for time integration of multiple time scale systems. *Journal of Computational Physics* 2003; **185**:583–611.
8. Evans KJ, Knoll DA, Pernice MA. Development of a 2-D algorithm to simulate convection and phase transition efficiently. *Journal of Computational Physics* 2006; **219**:404–417.
9. Patankar SV. *Numerical Heat Transfer and Fluid Flow*. Hemisphere: New York, 1980.
10. Brent AD, Voller VR, Reid KJ. Enthalpy porosity technique for modeling convection–diffusion phase change: application to the melting of a pure metal. *Numerical Heat Transfer* 1988; **13**:297–318.
11. Knoll DA, Keyes DE. Jacobian-free Newton–Krylov methods: a survey of approaches and applications. *Journal of Computational Physics* 2004; **193**:357–397.
12. Hairer E, Wanner G. *Solving Ordinary Differential–Algebraic Equations*. Springer: Berlin, 2002.
13. Evans KJ, Knoll DA, Pernice MA. Enhanced algorithm efficiency using a multigrid preconditioner and SIMPLE based smoother. *Journal of Computational Physics* 2007; **223**:121–126.
14. Stella F, Giangi M. Melting of a pure metal on a vertical wall: numerical simulation. *Numerical Heat Transfer A* 2000; **38**:193–208.
15. Morgan K. A numerical analysis of freezing and melting with convection. *Computer Methods in Applied Mechanics and Engineering* 1981; **28**:275–284.
16. Danzig JA. Modelling liquid–solid phase changes with melt convection. *International Journal for Numerical Methods in Engineering* 1989; **28**:1769–1785.
17. Voller VR, Cross M, Markatos NC. An enthalpy method for convection/diffusion phase change. *International Journal for Numerical Methods in Engineering* 1987; **24**:271–284.
18. Voller VR, Swaminathan CR, Thomas BG. Fixed grid technique for phase change problems: a review. *International Journal for Numerical Methods in Engineering* 1988; **30**:875–898.
19. Gau C, Vistanka R. Melting and solidification of a pure metal from a vertical wall. *Journal of Heat Transfer* 1986; **108**:171–174.

DOI: 10.1002/fld